Copper-Catalyzed Hydroquinone Oxidation and Associated Redox Cycling of Copper under Conditions Typical of Natural Saline Waters

ARTICLE *in* ENVIRONMENTAL SCIENCE & TECHNOLOGY · JUNE 2013

Impact Factor: 5.33 · DOI: 10.1021/es4014344 · Source: PubMed

4 AUTHORS:

Xiu Yuan
Lawrence Berkeley National Laboratory
5 PUBLICATIONS **30** CITATIONS
SEE PROFILE

An Ninh Pham
University of New South Wales
23 PUBLICATIONS **443** CITATIONS
SEE PROFILE

Christopher J Miller
University of New South Wales
17 PUBLICATIONS **219** CITATIONS
SEE PROFILE

T. David Waite
University of New South Wales
318 PUBLICATIONS **9,891** CITATIONS
SEE PROFILE

Environmental Science & Technology

Article

pubs.acs.org/est

Copper-Catalyzed Hydroquinone Oxidation and Associated Redox Cycling of Copper under Conditions Typical of Natural Saline Waters

Xiu Yuan, A. Ninh Pham, Christopher J. Miller, and T. David Waite*

School of Civil and Environmental Engineering, The University of New South Wales, Sydney, New South Wales 2052, Australia

Supporting Information

ABSTRACT: A detailed kinetic model has been developed to describe the oxidation of Cu(I) by O_2 and the reduction of Cu(II) by 1,4-hydroquinone (H_2Q) in the presence of O_2 in 0.7 M NaCl solution over a pH range of 6.5−8.0. The reaction between Cu(I) and O_2 is shown to be the most important pathway in the overall oxidation of Cu(I), with the rate constant for this oxidation process increasing with an increasing pH. In 0.7 M NaCl solutions, Cu(II) is capable of catalyzing the oxidation of H_2Q in the presence of O_2 with the monoanion, HQ^-, the kinetically active hydroquinone form, reducing Cu(II) with an intrinsic rate constant of $(5.0 \pm 0.4) \times 10^7$ M^{-1} s^{-1}. Acting as a chain-propagating species, the deprotonated semiquinone radical ($SQ^{\bullet -}$) generated from both the one-electron oxidation of H_2Q and the one-electron reduction of 1,4-benzoquinone (BQ) also reacts rapidly with Cu(II) and Cu(I), with the same rate constant of $(2.0 \pm 0.5) \times 10^7$ M^{-1} s^{-1}. In addition to its role in reformation of Cu(II) via continuous oxidation of Cu(I), O_2 rapidly removes $SQ^{\bullet -}$, resulting in the generation of $O_2^{\bullet -}$. Agreement between half-cell reduction potentials of different redox couples provides confirmation of the veracity of the proposed model describing the interactions of copper and quinone species in circumneutral pH saline solutions.

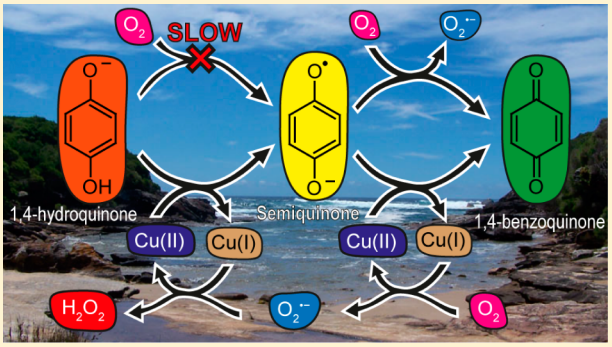

1. INTRODUCTION

Copper (Cu) is an essential transition metal that is involved in a variety of physicochemical reactions and physiological processes in natural aquatic systems. The oxidation of Cu(I) in marine systems has been extensively studied in recent decades,[1−5] principally because the redox transformations between cuprous copper [Cu(I)] and cupric copper [Cu(II)] species in the upper water column play a significant role in Cu transport and bioavailability.[6] Although required as a trace nutrient by all living organisms, copper in excess can be potentially toxic.[7,8] Currently, there is also concern regarding copper contamination of drinking waters as a result of the widespread use of copper in water supply pipes.[9−12] Copper is also important in human health, with this element distributed throughout the human body but with significant storage in the liver and bone marrow.[13] Studies focused on the potential roles of copper as a mediator of reactive-oxygen-species-induced cytotoxicity and genotoxicity have attracted particular interest.[14−19] For example, Li and Trush,[17,19] in studies of the ability of copper−quinone mixtures to cleave DNA, have demonstrated that Cu(II) is capable of oxidizing 1,4-hydroquinone (H_2Q), resulting in the formation of the semiquinone anion radical ($SQ^{\bullet -}$), benzoquinone (BQ), and hydrogen peroxide (H_2O_2) through an oxidant-producing copper-redox cycle mechanism. The addition of Cu(II) to primary bone marrow stromal cell cultures has also been shown to significantly enhance H_2Q-induced cytotoxicity.[19]

The term quinone collectively refers to organic structures in three oxidation states, with one electron reduction of a quinone forming a semiquinone radical, which can be further reduced to the hydroquinone form. These species are common constituents of many biologically relevant molecules and serve as a vital link in the movement of electrons through cells and tissues.[20] As electron-transfer mediators, quinone moieties in natural organic matter (NOM) play important roles in essential biogeochemical processes, with these redox active compounds arising from the degradation and biological reworking of plant tissue.[21−24] The free radical content of NOM, observed using techniques such as electron paramagnetic resonance (EPR) spectroscopy,[24−26] has been attributed to the generation of semiquinone radicals.[25,27,28]

The ability of copper to catalyze the oxidation of hydroquinone has been verified in several studies,[17−19,29] with concomitant formation of benzoquinone and H_2O_2. However, no kinetic rate constants between copper and the quinone species have been reported. Additionally, many of the previous ligand-free studies have used high concentrations of Cu(II),[17,19] which may have resulted in the precipitation of Cu(II) under such conditions.

Received: April 2, 2013
Revised: June 18, 2013
Accepted: June 24, 2013
Published: June 24, 2013

   dx.doi.org/10.1021/es4014344 | Environ. Sci. Technol. 2013, 47, 8355−8364

In this study, the oxidation of inorganic Cu(I) over the pH range of 6.5−8.0 is first considered, with emphasis on the development of a condition-specific kinetic description of the mechanism of oxidation of Cu(I). Using results from the inorganic system as a basis, this modeling approach is then extended to the description of the kinetics of copper transformations in the presence of H_2Q. Using the derived kinetic model, thermodynamic characteristics of the system are deduced, with agreement between the half-cell reduction potentials of different redox couples presented as evidence for the veracity of the proposed kinetic model.

2. MATERIALS AND METHODS

A complete description of the materials and methods used appears in SI1 of the Supporting Information.

2.1. Reagents. All solutions were prepared in 0.7 M NaCl (puriss, >99.8%) and 2 mM $NaHCO_3$. 3-(*N*-Morpholino)-propanesulfonic acid (MOPS) (2 mM) was used to control the pH over the range of 6.5−8.0 because it was found to have a negligible effect on the redox reactions of copper (see Figure S1 in SI1 of the Supporting Information) [*N*-2-hydroxyethylpiperazine-*N*′-2-ethanesulfonic acid (HEPES), 2-(*N*-morpholino)-ethanesulfonic acid (MES), and phosphate buffers were also trialed but found to interfere with the system]. Solution pH was adjusted by adding 1 M HCl or 1 M NaOH to reaction mixtures. Tris-(hydroxymethyl)aminomethane was employed to calibrate the pH electrode on the free hydrogen ion scale.[30] All pH measurements were conducted using a Hanna 210 microprocessor pH meter combined with a glass electrode and Ag/AgCl reference.

Cu(I) stock solutions (0.4 mM) were prepared daily according to the method described previously.[1] Cu(II) stock solutions (20 mM) were prepared weekly by dissolving an appropriate amount of copper(II) chloride in 5 mM HCl solution. Stock solutions of H_2Q were prepared daily in 5 mM HCl solution in the presence of 100 nM diethylenetriaminepentaacetic acid (DTPA). The acidic condition ensured that the deterioration of H_2Q during 1 day of storage was negligible, while DTPA was used to eliminate the possible effect of trace-metal contamination in the solutions. The concentration of DTPA in the stock solution was also sufficiently low that the interaction between copper and DTPA is negligible upon addition of the H_2Q stock to experimental solutions at dilution factors of 10^3−10^4.

2.2. Experimental Measurement. *2.2.1. Measurement of BQ.* The concentrations of BQ were determined by its absorbance at 247 nm using a Cary 50 spectrophotometer (Varian, Inc.), with $\varepsilon_{max} = 2.53 \times 10^4$ M^{-1} cm^{-1}.[19]

2.2.2. Cu(I) Determination. Cu(I) concentrations were determined spectrophotometrically using the bathocuproine (BC) method.[1,31]

2.2.3. H_2O_2 Determination. H_2O_2 concentrations were measured using the Amplex Red method.[32]

2.2.4. System Redox Potential (E_h) Determination. Open circuit chronopotentiometric measurements were carried out to determine E_h of the system using the same electrochemical workstation described elsewhere.[33]

Further details of the measurement methods used are provided in SI1 of the Supporting Information.

2.3. Kinetic Modeling. The kinetic model was fitted to the experimental data over a range of experimental conditions using the program Kintek Explorer.[34] The sensitivity of the model to changes in individual rate constant values was also assessed by examining the change in the relative difference between the experimental data and the kinetic model (defined as the relative residual, *r*) when one rate constant was varied while holding the others fixed at their optimal values. The program Kintecus[35] was employed to evaluate the kinetic model using a Visual Basic for Applications (VBA) program to calculate *r* (see detailed description and Figure S2 in SI2 of the Supporting Information).

3. RESULTS AND DISCUSSION

3.1. Cu(I) Oxidation by O_2. The oxidation of 200 and 400 nM of Cu(I) in 0.7 M NaCl solutions over the pH range of 6.5−8.0 has been investigated, with results shown in Figure 1.

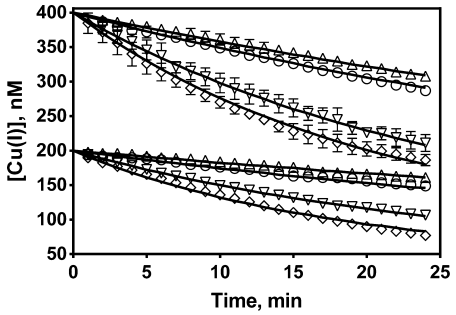

Figure 1. Oxidation of Cu(I) in 0.7 M NaCl at (△) pH 6.5, (○) pH 7.0, (▽) pH 7.5, and (◇) pH 8.0 with $[Cu(I)]_0$ = 200 and 400 nM. Error bars (some of which are too small to be visible) are the standard errors from triplicate measurements, and solid lines represent the model fit using reactions 1−3 (Table 1).

As observed in previous studies,[1−5] the oxidation rate increased with an increasing pH, with this effect attributed to the involvement of pH-dependent cuprous species in the overall oxidation.[1] Further, it has been reported that different Cu(I) species, such as Cu^+, $CuCl_{(aq)}$, and $CuCl_2^-$ react with O_2 and $O_2^{\bullet -}$ at very different rates.[2−4,36,37] As such (and as performed in our previous study[1]), different oxidation reactions for each of the various cuprous species should ideally be included in the model, with individual rate constants ascribed to each reaction. However, in natural waters and biological fluids, the variety of potential copper-binding ligands is large, rendering determination of the actual Cu(I) and Cu(II) species present difficult and elucidation of rate constants for reactions of these species (and subsequent development of a unique kinetic model describing transformations of individual species) essentially impossible.[38] Hence, in this study, the oxidation of inorganic Cu(I) is modeled using an approach similar to that developed for description of Fe(II) oxidation by Rose and Waite[39] (the "FeL approach"). This alternate approach of defining Cu(I) and Cu(II) as single entities to represent all cuprous and cupric species present in a specific, well-defined system possesses the advantage of being much simpler and, as noted above, has been employed successfully for the modeling of Fe(II) oxidation[38,39] and Cu(II) reduction.[40]

A list of reactions considered in this model with corresponding rate constants is presented in Table 1. Similar to our previous work,[1,40,41] the reported rate constants for the reaction of $O_2^{\bullet -}$ with Cu(I) and Cu(II) (reactions 2 and 3 in Table 1), $k_2 = 1.98 \times 10^9$ M^{-1} s^{-1} and $k_3 = 6.63 \times 10^8$ M^{-1} s^{-1},[37] were employed and remained constant at all pH values considered here. Reactions between Cu(I)/Cu(II) and H_2O_2, together with other possible reactions in this system, were not

dx.doi.org/10.1021/es4014344 | Environ. Sci. Technol. 2013, 47, 8355−8364

Table 1. Modeled Reactions and Rate Constants for the Cu(I) Oxidation[a]

number	reaction	rate constant (M^{-1} s^{-1}) pH	6.5	7.0	7.5	8.0	reference
		k_{app}[b]	0.75 ± 0.09	0.94 ± 0.07	1.9 ± 0.1	2.7 ± 0.4	this study
1	$Cu(I) + O_2 \rightarrow Cu(II) + O_2^{\bullet -}$	k_1[c]	0.35 ± 0.01	0.48 ± 0.01	1.00 ± 0.01	1.50 ± 0.03	
2	$Cu(I) + O_2^{\bullet -} \xrightarrow{+2H^+} Cu(II) + H_2O_2$			1.98×10^9			37
3	$Cu(II) + O_2^{\bullet -} \rightarrow Cu(I) + O_2$			6.63×10^8			37

[a]In general, the overall oxidation rate of Cu(I) can be described by $-d[Cu(I)]/dt = k_{app}[O_2][Cu(I)]$, where [Cu(I)] is the total or analytical Cu(I) concentration and k_{app} (M^{-1} s^{-1}) is the apparent oxidation rate constant. In oxygen-saturated systems (where $[O_2] \gg [Cu(I)]$), the initial decay of Cu(I) was observed to follow pseudo-first-order kinetics with a rate constant $k' = k_{app}[O_2]_0$. [b]Values of k_{app} were calculated given an O_2 concentration of 0.243 mM[42] under the experimental conditions used. [c]k_1 is the intrinsic rate constant for reaction 1, the one-electron-transfer step, yielding $O_2^{\bullet -}$.

Table 2. Modeled Reactions and Rate Constants of Cu(II) Reduction in the Presence of H_2Q

number	reaction	rate constant (M^{-1} s^{-1})[a]	reference
4	$H_2Q^0 \rightleftharpoons HQ^- + H^+$	$K_{a1} = 10^{-10.16}$ M	27
5	$HQ^- \rightleftharpoons Q^{2-} + H^+$	$K_{a2} = 10^{-12.02}$ M	27
6	$HQ^- + Cu(II) \underset{(+H^+),k_{-6}}{\overset{(-H^+),k_6}{\rightleftharpoons}} Cu(I) + SQ^{\bullet -}$	$k_6 = (5.0 \pm 0.4) \times 10^7$, $k_{-6} = (2.0 \pm 0.5) \times 10^7$	this study
7	$Cu(II) + SQ^{\bullet -} \underset{k_{-7}}{\overset{k_7}{\rightleftharpoons}} Cu(I) + BQ$	$k_7 = (2.0 \pm 0.3) \times 10^7$, $k_{-7} = 150-300$	this study
8	$SQ^{\bullet -} + O_2 \underset{k_{-8}}{\overset{k_8}{\rightleftharpoons}} BQ + O_2^{\bullet -}$	$k_8 = 5.0 \times 10^4$, $k_{-8} = 1.0 \times 10^9$	53 and 54
9	$Q^{2-} + BQ \underset{k_{-9}}{\overset{k_9}{\rightleftharpoons}} SQ^{\bullet -} + SQ^{\bullet -}$	$k_9 = 4.0 \times 10^9$, $k_{-9} = 8.0 \times 10^7$	44, 47, and 55
10	$Cu(II) + H_2O_2 \xrightarrow{-2H^+} Cu(I) + O_2^{\bullet -}$	460[b]	40 and 41

[a]Unless noted otherwise. [b]This reaction was only included at pH 8.0.

important and, thus, were excluded from the model (see detailed analysis in SI3 of the Supporting Information). Results of model fitting for the oxidation of Cu(I) by O_2 in 0.7 M NaCl over the pH range of 6.5−8.0 using reactions 1−3 (Table 1) are illustrated in Figure 1 (with only k_1 as the fitting parameter).

In general, the model provides excellent fits to the experimental data (Figure 1). The general agreement between the model output and the experimental data supports the proposed mechanism, assignment of rate constants, and more importantly, the modeling approach. As shown in Table 1, oxidation of Cu(I) by O_2 was found to be the rate-limiting step, with the intrinsic rate constant k_1 increasing with an increasing pH, consistent with the previous conclusions by Moffett and Zika[36] and in accordance with results of our previous studies, where the concentrations of $CuClOH^-$ and $CuCO_3^-$ [key species involved in the oxidation of Cu(I)] were recognized to increase with an increasing pH.[1] Furthermore, over the range of conditions used in this work, k_1 is approximately 50% of k_{app}, indicating that O_2 oxidizes copper with a stoichiometry of 1:2, with the $O_2^{\bullet -}$ formed during reaction 1 predominantly oxidizing additional Cu(I) under the conditions of this work {at least initially when [Cu(I)] > [Cu(II)], where back-reduction of Cu(II) by $O_2^{\bullet -}$ (reaction 3) is unimportant}. It is clear that H_2O_2 formed in reaction 2 (Table 1) does not build up to concentrations high enough to significantly oxidize Cu(I) or reduce Cu(II), with the ability of the model considering only reactions 1−3 to fit the data justifying the exclusion of these slow H_2O_2-mediated processes.

3.2. Cu(II) Reduction in the Presence of Hydroquinone. The autoxidation of H_2Q is spin-restricted and extremely slow under natural conditions (see Figure S3 in SI4 of the Supporting Information), but this process can be significantly accelerated by transition-metal catalysts, which overcome this spin restriction. Copper, as one of the major redox-active transition metals in natural systems, has been shown to serve as a catalyst for the oxidation of hydroquinones.[17−19,29] In this study, the oxidation of H_2Q in the presence of copper under aerobic conditions in 0.7 M NaCl has been investigated between pH 6.5 and 8.0. In addition, considering the possible interference caused by the trace amounts of adventitious transition metals in the reaction solutions, the extent of metal contamination was investigated. Based on the model prediction (Tables 1 and 2), it was found to be equivalent to 2 ± 0.3 nM Cu(II) (see details in SI4 of the Supporting Information). In most of the experiments described here, the initial concentration of Cu(II) ($[Cu(II)]_0$) employed for H_2Q oxidation was more than 100 nM; thus, the interference from the metal contamination in our background solution was considered to be negligible. However, at pH 8.0, this "background" interference becomes important at low added $[Cu(II)]_0$; under these conditions, it was assumed that contaminants equivalent to $[Cu(II)]_0$ of 2 nM were present, with model fits obtained with this assumption shown in Figure 2D.

3.2.1. Cu(II) Reduction and H_2Q Oxidation. The effects of pH and $[Cu(II)]_0$ on the oxidation of H_2Q were initially investigated, with the results presented in Figure 2. As seen

dx.doi.org/10.1021/es4014344 | Environ. Sci. Technol. 2013, 47, 8355−8364

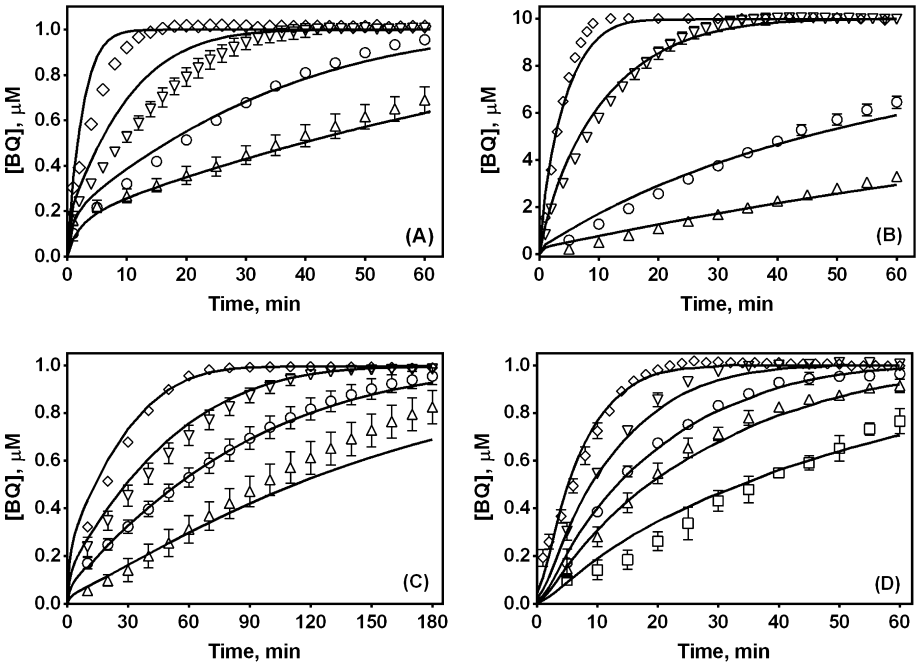

Figure 2. pH and $[Cu(II)]_0$ dependence upon Cu(II)-catalyzed oxidation of H_2Q in 0.7 M NaCl. Solid lines represent the model fit using reactions 1−10 (Tables 1 and 2). Error bars (some of which are too small to be visible) are the standard errors from triplicate measurements. (A) $[Cu(II)]_0$ = 200 nM and $[H_2Q]_0$ = 1.0 μM, at (△) pH 6.5, (○) pH 7.0, (▽) pH 7.5, and (◇) pH 8.0; (B) $[Cu(II)]_0$ = 200 nM and $[H_2Q]_0$ = 10 μM, at (△) pH 6.5, (○) pH 7.0, (▽) pH 7.5, and (◇) pH 8.0; (C) pH 7.0 and $[H_2Q]_0$ = 1.0 μM, with $[Cu(II)]_0$ of (△) 20 nM, (○) 50 nM, (▽) 100 nM, and (◇) 200 nM; and (D) pH 8.0 and $[H_2Q]_0$ = 1.0 μM, with added $[Cu(II)]_0$ of (□) 0 nM, (△) 2 nM, (○) 4 nM, (▽) 8 nM, and (◇) 20 nM, with each fitted $[Cu(II)]_0$ being 2 nM higher than the added $[Cu(II)]_0$ because the background contamination was only considered at pH 8.0.

from panels A and B of Figure 2, the rate of oxidation of H_2Q in the presence of Cu(II) increased significantly with an increasing pH. For example, in the presence of 200 nM $[Cu(II)]_0$, 10 μM H_2Q was nearly completely oxidized in the first 10 min at pH 8.0, while less than 10% of H_2Q initially present was oxidized at pH 6.5 (Figure 2B). The pH dependence of hydroquinone oxidation and the reduction of cytochromes and ferric iron by hydroquinones have been investigated in a variety of previous studies.[43−48] Some reported that the rate constant was proportional to $[H^+]^{-2}$, while others observed proportionality with $[H^+]^{-1}$. However, Song and Buettner[20] indicated that the rate law for the O_2-mediated oxidation of hydroquinone is second-order with respect to H^+ (i.e., proportional to $[H^+]^{-2}$), whereas in metal-catalyzed oxidations, the rate law is often first-order (i.e., proportional to $[H^+]^{-1}$), indicating that different species are likely to be involved in these different routes of oxidation. Detailed analysis of the pH dependence of Cu(II) reduction by H_2Q is provided in the next section.

As shown in panels C and D of Figure 2, the oxidation of H_2Q was greatly accelerated by increasing $[Cu(II)]_0$. It should also be noted that, under aerobic conditions, even in the presence of only 20 nM $[Cu(II)]_0$, almost 800 nM H_2Q was oxidized to BQ within 3 h at pH 7.0, while at pH 8.0, complete oxidation of 1000 nM H_2Q was observed in less than 20 min for $[Cu(II)]_0$ of 20 nM, indicating that Cu(II) catalyzed the overall oxidation of H_2Q in a strongly pH-dependent manner.

In view of its catalytic role, the transformation of copper in the system is also of great interest. A direct measurement of Cu(I) concentrations over a range of conditions was undertaken to assist in determining the mechanism and constraining the fitting parameters. The corresponding results are shown in Figures 3 and 4 and S4 of the Supporting Information. As

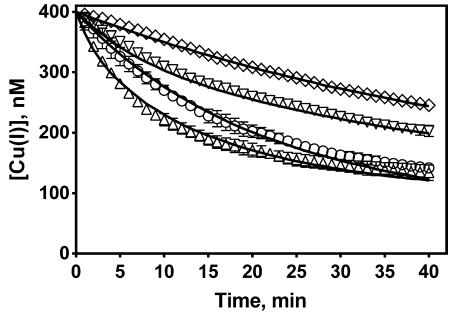

Figure 3. Oxidation of Cu(I) in the absence and presence of BQ with $[Cu(I)]_0$ = 400 nM and (◇) pH 7.0, without BQ; (▽) pH 7.0, $[BQ]_0$ = 1.0 μM; (○) pH 8.0, without BQ; and (△) pH 8.0, $[BQ]_0$ = 1.0 μM. Error bars (some of which are too small to be visible) are the standard errors from triplicate measurements, and solid lines represent the model fit using reactions 1−10 (Tables 1 and 2).

shown in Figure 3, the presence of 1.0 μM BQ moderately enhanced the oxidation of Cu(I), although at later stages of the reaction (after 20 min), the enhancement declined slightly with an increasing pH, suggesting that the oxidation of Cu(I) by BQ is not important compared to the oxidation of Cu(I) by O_2 at higher pH.

When Cu(I) is oxidized by O_2 in the presence of H_2Q, four distinct phases of oxidation are observed (Figure 4). For example, with $[Cu(I)]_0$ = 400 nM, there is an abrupt decrease of [Cu(I)] in the initial 2 min, with this decrease initiated by the oxidation of Cu(I) by O_2, yielding Cu(II) and $O_2^{\bullet -}$ (reaction 1 in Table 1). For each mole of Cu(I) oxidized by O_2, a rather slow process, a cascade of further rapid Cu(I) oxidation ensues, with Cu(II) thus formed serving to further accelerate this oxidation. This rapid oxidation phase is followed

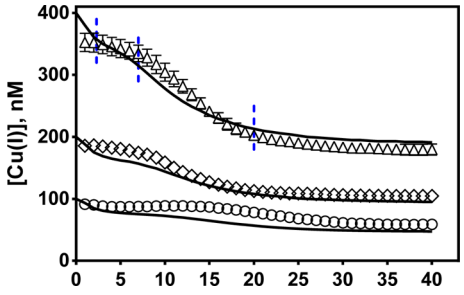

Figure 4. Oxidation of Cu(I) in the presence of H_2Q at pH 8.0, $[H_2Q]_0$ = 1.0 μM, and (△) $[Cu(I)]_0$ = 400 nM, (◇) $[Cu(I)]_0$ = 200 nM, and (○) $[Cu(I)]_0$ = 100 nM. Error bars (some of which are too small to be visible) are the standard errors from triplicate measurements, and solid lines represent the model fit using reactions 1−10 (Tables 1 and 2). Dashed lines are provided as indicators of the different oxidation phases.

by a period of pseudo-equilibrium between Cu(I) and Cu(II) (around 3−7 min) attributed to the build up of Cu(II) in the system, with a balance between reduction of Cu(II) by H_2Q and oxidation of Cu(I) by $O_2^{\bullet -}$ and $SQ^{\bullet -}$ reached. According to the kinetic model, in the presence of 400 nM $[Cu(I)]_0$, 1.0 μM H_2Q was near-completely oxidized to BQ after ∼7 min (see Figure S5 in SI5 of the Supporting Information), from which point [Cu(I)] decreased quickly (8−20 min) simply because the reduction of Cu(II) by H_2Q ceased and the oxidation of Cu(I) by O_2 became predominant again. Subsequently, the decline of [Cu(I)] became increasingly slow, with [Cu(I)] approaching steady state as the balance between Cu(I) oxidation and Cu(II) reduction was finally reached.

To gain some insight into the transformation of Cu(II) and Cu(I) in the system, the cycling rate and turnover frequency of copper have been calculated using the kinetic model, with detailed description and results (see Figures S6 and S7 of the Supporting Information) provided in section SI6 of the Supporting Information. As an example, for the case of 200 nM Cu(I) and 10 μM H_2Q at pH 8.0, in the period before t = 15 min, significant cycling between Cu(I) and Cu(II) occurs, peaking at around t = 0.5 min, with a turnover frequency of ∼1080 h^{-1}. This highly dynamic region is only short-lived and reverts rapidly to a much smaller turnover frequency of only about 20 h^{-1}. The results suggest that the rapid cycling of copper is driven primarily by the $H_2Q/SQ^{\bullet -}/BQ$ system, with some significant influence of the $O_2/O_2^{\bullet -}$ system. Overall, in the presence, for example, of 200 nM Cu(I) and 10 μM H_2Q at pH 8.0, copper is cycled approximately 95 times in the first 12 min, with a further 17 cycles occurring from t = 12 to 60 min.

The results of previous studies also suggested that, during the Cu(II)-catalyzed oxidation of H_2Q, stoichiometric amounts of hydrogen peroxide (H_2O_2) will be generated.[17−19,29] H_2O_2 is of particular interest because it is ubiquitous in both the cells of organisms as a byproduct of oxygen metabolism and surface seawater primarily as a result of photochemical processes mediated by NOM[49] and may lead to the formation of highly reactive and damaging oxidants, such as the hydroxyl radical ($HO^{\bullet}$),[50] or, in a system containing copper, high valence Cu species [such as Cu(III)].[41] Therefore, the generation of H_2O_2 at different pH values was also investigated, with results shown in Figure 5. The data are in good agreement with the previous prediction that the oxidation of H_2Q results in the stoichiometric production of H_2O_2 (Figure 5) and BQ (Figure 2A).[20,51,52]

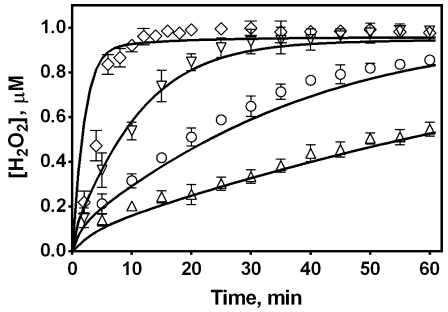

Figure 5. Generation of H_2O_2 by Cu(II) reduction of H_2Q, $[H_2Q]_0$ = 1.0 μM, and $[Cu(II)]_0$ = 200 nM at (◊) pH 8.0, (▽) pH 7.5, (○) pH 7.0, and (△) pH 6.5. Error bars (some of which are too small to be visible) are the standard errors from triplicate measurements, and solid lines represent the model fit using reactions 1−10 (Tables 1 and 2).

3.2.2. Kinetic Model for Cu(II) Reduction in the Presence of H_2Q. When H_2Q is present, in addition to the reactions presented in Table 1, reactions describing the electron transfer between copper and quinone species and between the semiquinone radical and oxygen and the comproportionation/disproportionation of different quinone species should also be included. The additional reactions considered in the model and corresponding rate constants are listed in Table 2, with all reactions listed in Table 1 also occurring in the system.

As previously stated, the oxidation of H_2Q by O_2 is extremely slow because of spin restrictions and is negligible at neutral pH; thus, it was not included in the model.[52,56] However, the semiquinone intermediate generated from the one-electron oxidation of hydroquinone or one-electron reduction of benzoquinone is a substantially more facile electron donor to O_2, with the one-electron reduction of O_2 resulting in the formation of $O_2^{\bullet -}$, as shown electrochemically by Tatsumi et al.[57] Therefore, reaction 8, including the forward and backward reactions (Table 2), was included using previously reported rate constants,[53,54,56,58] $k_8 = 5.0 \times 10^4$ M^{-1} s^{-1} and $k_{-8} = 1.0 \times 10^9$ M^{-1} s^{-1}. The equilibrium constant (K) of reaction 8 can also be determined by the standard reduction potential (E^0) of both redox couples ($BQ/SQ^{\bullet -}$ and $O_2/O_2^{\bullet -}$) using the Nernst equation:[59]

$$E^0_{(O_2/O_2^{\bullet -})} - E^0_{(BQ/SQ^{\bullet -})} = \frac{RT}{nF} \ln K \quad (1)$$

where R is the gas constant in appropriate units, 8.314 J K^{-1} mol^{-1}, T is the temperature in Kelvin, F is the Faraday constant, 9.6485 × 10^4 C mol^{-1}, and n is the number of electrons involved in the reaction. Thus, when n = 1, at 25 °C, eq 1 can be written as

$$\log K = \frac{E^0_{(O_2/O_2^{\bullet -})} - E^0_{(BQ/SQ^{\bullet -})}}{0.059} \quad (2)$$

Here, we employed the values of $E^0(O_2/O_2^{\bullet -}) = -0.18$ V[60,61] and $E^0(BQ/SQ^{\bullet -}) = 0.078$ V[22,62] in eq 2 to calculate $K = 4.3 \times 10^{-5}$, which is in good agreement with $K_8 = k_8/k_{-8} = 5.0 \times 10^{-5}$ used in this study.

The comproportionation between H_2Q and BQ and the disproportionation of $SQ^{\bullet -}$ were included as reaction 9 (Table 2). This reaction has been investigated in detail in other

dx.doi.org/10.1021/es4014344 | Environ. Sci. Technol. 2013, 47, 8355−8364

studies.[44,47,55,62,63] For the comproportionation reaction, the doubly dissociated hydroquinone (Q^{2-}) plays a dominant role in the generation of semiquinone at neutral pH, with a rate constant of 6.3×10^8 M^{-1} s^{-1},[47] which is close to the value of 2.6×10^8 M^{-1} s^{-1} reported by Von Diebler et al.[55] Yamazaki and Ohnishi[44] also determined the apparent rate constant of $SQ^{\bullet -}$ formation from the comproportionation between H_2Q and BQ to be 5.8 M^{-1} s^{-1} at pH 6.5. On the basis of the acidity constants of H_2Q used in this study (pK_{a1} = 10.16 and pK_{a2} = 12.02),[20,27] the rate constant for reaction 9 can be calculated as 8.8×10^9 M^{-1} s^{-1}. According to these previously reported values and the model fitting, a value of 4.0×10^9 M^{-1} s^{-1} was adopted here. In the same studies,[44,47] the rate constant of the reverse reaction (k_{-9}), 8.0×10^7 M^{-1} s^{-1}, was shown to be pH-independent near neutral pH because the acidity constant of *p*-semiquinone is around pH 4.1, suggesting that the dissociated semiquinone (i.e., $SQ^{\bullet -}$) is the kinetically active form.[27] This value is similar to that reported in several other studies.[55,64,65] Furthermore, as indicated in the study by Uchimiya and Stone,[22] the equilibrium constant for the comproportionation between BQ and Q^{2-} can be readily deduced as shown below:

$$BQ + e^- = SQ^{\bullet -}, \qquad E^0 = 0.078\ V$$

$$SQ^{\bullet -} + e^- = Q^{2-}, \qquad E^0 = 0.024\ V$$

$$\text{overall: } BQ + Q^{2-} = SQ^{\bullet -} + SQ^{\bullet -}, \quad E^0 = 0.054\ V$$

Thus

$$\log K_{\text{comproportionation}} = \frac{E^0_{(BQ/SQ^{\bullet -})} - E^0_{(SQ^{\bullet -}/Q^{2-})}}{0.059} = 0.92 \tag{3}$$

The values adopted in the present study give $K_9 = (k_9)/(k_{-9}) = 10^{1.7}$, which is reasonably close to $10^{0.92}$, validating the assignment of rate constants in this study.

As H_2Q is oxidized to BQ, a near-stoichiometric quantity of H_2O_2 is also formed; thus, as shown in Table 2, the reduction of Cu(II) by H_2O_2 was included in the kinetic model as reaction 10 (the reverse of reaction 2 in Table 1). This reaction was only included in the model at pH 8.0 because it exerted a negligible effect on the fitting in the pH range of 6.5−7.5 when the rate constant (k_{10}) was varied in the reasonable range of 0−500 M^{-1} s^{-1} reported previously.[36,66] However, at pH 8.0 under the conditions used in Figure 4, this reaction shows some mild influence in the latter stage (from 15 min on) on the steady-state concentration of Cu(I). This is because the concentration of H_2O_2 in the system, as shown in Figure 5, approaches 1.0 μM when 1.0 μM H_2Q is completely oxidized to BQ. This H_2O_2 concentration is over an order of magnitude higher than that generated in the Cu(I)−O_2 system (Table 1), which enables the back reduction of Cu(II) by H_2O_2 to influence the kinetics of oxidation of Cu(I), because $k_{10}[Cu(II)][H_2O_2]$ becomes relatively comparable to $k_{app}[O_2][Cu(I)]$. On the basis of the previously reported value,[40,41,66] we have assigned k_{10} = 460 M^{-1} s^{-1} at pH 8.0. Although additional profiles of [Cu(I)] as a function of time (similar to Figure 4) over the pH range of 6.5−7.5 might be helpful in constraining k_{10}, the model is relatively insensitive to this reaction given its minimal importance at lower pH, because the rate constant has been reported to decrease with a decreasing pH.[36,66] As indicated in previous studies,[41,67,68] H_2O_2 could also react with Cu(I) and $SQ^{\bullet -}$, resulting in the formation of Cu(III) and $HO^{\bullet}$, respectively. However, because of the relatively low rate and on the basis of the model prediction, the generation of these highly reactive oxidants in this system is insufficient to play any important role (see details in SI7 of the Supporting Information), and therefore, these reactions were not included in the model.

As indicated in the study by Eyer,[56] the oxidation of H_2Q by superoxide was not expected to be significant in our system given the relatively low reaction rate constant of $\leq 10^4$−10^5 M^{-1} s^{-1}.[52,69,70] This was also verified by the result that inclusion of this reaction in the kinetic model and varying the rate constant from 10 to 10^7 M^{-1} s^{-1} had a negligible effect on the model fitting (see sensitivity analysis and Figure S2A in SI2 of the Supporting Information). As such, this reaction was not included here. Additionally, the cross-dismutation between $SQ^{\bullet -}$ and $O_2^{\bullet -}$ might also occur; however, little information on this reaction has been previously reported, and the rate constant is not known. Inclusion of this reaction in simulations and varying the rate constant over a reasonable range revealed minimal effect on the fitting (see Figure S2B in SI2 of the Supporting Information), justifying exclusion of this reaction from the model. A self-exchange reaction between $SQ^{\bullet -}$ and its parent BQ (eq 4) also occurs with a rate constant of $(6.2 \pm 0.5) \times 10^7$ M^{-1} s^{-1}.[71]

$$SQ^{\bullet -} + BQ \rightleftharpoons BQ + SQ^{\bullet -} \tag{4}$$

However, because the self-exchange reaction does not exert any influence on the overall system, it was not given further consideration here.

Because of the limited information available in the literature, rate constants for the interaction of copper and quinone species (reactions 6 and 7 in Table 2) were determined empirically by the best fit of the model to the experimental data. Results of model fitting in 0.7 M NaCl over the pH range of 6.5−8.0 using reactions 1−10 (Tables 1 and 2) are illustrated in Figures 2−5. In general, the model provides reasonable fits to the experimental data over a range of conditions. The good agreement between the model output and the experimental data validates our assumptions of the proposed mechanism and the assignment of rate constants.

3.2.3. Thermodynamic Considerations Relating to the Reduction of Cu(II) by H_2Q. At neutral pH, 1,4-hydroquinone mainly exists in its undissociated form (H_2Q^0), with monodissociated (HQ^-) and doubly dissociated (Q^{2-}) anions being minor species because of its high acidity constants (pK_{a1} = 10.16, and pK_{a2} = 12.02).[20,27] However, in this study, HQ^- was found to be the kinetically active species toward Cu(II) reduction, with an intrinsic rate constant of $(5.0 \pm 0.4) \times 10^7$ M^{-1} s^{-1} over the pH range of 6.5−8.0, in agreement with the findings by Baxendale et al.,[48] who suggested that HQ^- is the species active in reducing ferric ion. Song and Buettner[20] also postulated that in metal-catalyzed oxidations of hydroquinones, the rate law is first-order in [OH^-], indicating that instead of the undissociated form H_2Q^0, the monoanion HQ^- is the important species in this redox route. Although HQ^- only occupies a small fraction of the total hydroquinone species at neutral pH, the rate of protonation/deprotonation equilibration is much faster than that of the redox reactions and, thus, is not rate-limiting.[45,72]

Rich and Bendall[45] also indicated that HQ^- is a much better reductant than the uncharged hydroquinone, H_2Q^0. This can be rationalized thermodynamically in terms of the calculated reduction potentials of the appropriate electron-transfer couples:[22]

$$SQ^{\bullet -} + 2H^+ + e^- = H_2Q^0, \quad E^0 = 1.335\ V,$$
$$\Delta G^0 = -nFE^0 = -128.81\ kJ\ mol^{-1}$$

$$H_2Q^0 = HQ^- + H^+, \quad K_{a1} = 10^{-10.16},$$
$$\Delta G^0 = -RT\ \ln K = 57.99\ kJ\ mol^{-1}$$

$$\text{overall: } SQ^{\bullet -} + H^+ + e^- = HQ^-,$$
$$\Delta G^0 = -70.82\ kJ\ mol^{-1},$$
$$E^0\ (SQ^{\bullet -}/HQ^-) = 0.734\ V$$

Therefore, the standard reduction potential of the $SQ^{\bullet -}/HQ^-$ couple is ~0.6 V lower than that of the $SQ^{\bullet -}/H_2Q^0$ couple, indicating that HQ^- is substantially more readily oxidized than H_2Q^0. Nevertheless, this standard midpoint potential is still much higher than that of the various Cu(II) species, such as Cu^{2+} and $CuCO_{3(aq)}$, which are the two major Cu(II) species present in this system[36] (see Table S1 and Figure S8 in SI8 of the Supporting Information), suggesting that reaction 6 (Table 2) is energetically unfavorable. However, it is important to recognize that the reduction potential of the $SQ^{\bullet -}/HQ^-$ couple exhibits strong pH dependency, with a slope of −59 mV (pH unit)$^{-1}$ (see detailed calculations in SI9 of the Supporting Information).[27,44,73,74] On the basis of the model prediction, the range of $E(SQ^{\bullet -}/HQ^-)$ in our system is 0.34−0.25 V with respect to the pH range of 6.5−8.0 (see Figure S9 in SI9 of the Supporting Information), which dramatically improves the feasibility of reaction 6. Moreover, the rapid removal of the product, $SQ^{\bullet -}$, by Cu(II) and O_2 (reactions 7 and 8, respectively) is another significant force driving reaction 6 to the right.[20,45] Thus, the presence of O_2 in the system not only acts to supply Cu(II) by continuously oxidizing Cu(I) but also induces the rapid removal of $SQ^{\bullet -}$, with resultant generation of $O_2^{\bullet -}$.

Detailed analysis of the predicted rate constants for the reactions between $SQ^{\bullet -}$ and Cu(I)/Cu(II) (k_{-6} and k_7, respectively) and between BQ and Cu(I) (k_{-7}) are provided in section SI10 of the Supporting Information. Despite the capability of the kinetic model in providing a good description of the various reactions between Cu(I), Cu(II), O_2, and the quinone triad (BQ, $SQ^{\bullet -}$, and H_2Q) over a range of experimental conditions with a relatively well-constrained set of rate constants, the model is limited by the assumption that the composite terms Cu(I) and Cu(II) adequately represent all inorganic copper in their +1 and +2 oxidation states, respectively. Therefore, care must be taken when interpreting the model results because the model, by default, is condition-specific. For example, the presence of chloride will influence the reactivity of various copper species, and as such, the composite "intrinsic" rate constants of various reactions with copper will need to be re-evaluated.

When oxidizing and reducing systems have come to a state of true equilibrium, the two systems will have the same redox potential. Therefore, estimation of the solution redox potentials and of particular individual redox couples may assist in ascertaining the likely tendency of proposed chemical reactions to occur under the conditions of the system being investigated.[40] For example, as shown in Figure 4, at pH 8.0 and with initial $[H_2Q]_0$ = 1.0 μM and $[Cu(I)]_0$ = 200 nM, a steady-state concentration of Cu(I) of ~100 nM was attained after 30 min of reaction; thus, the equilibrium redox potential of the whole system can be determined from the Cu^{2+}/Cu^+ couple. Speciation calculations with stability constants of various Cu(I) species tabulated in our previous study[1] at [Cu(I)] = 100 nM in 0.7 M NaCl and 2 mM $NaHCO_3$ using the program Visual MINTEQ[75] yielded $[Cu^+] = 7.82 \times 10^{-13}$ M, whereas the concentration of Cu^{2+} with [Cu(II)] = 100 nM was calculated to be 8.61×10^{-9} M at pH 8.0. Thus, the equilibrium redox potential of the system, assumed to be similar to that of the Cu^{2+}/Cu^+ couple, is given by the Nernst equation:

$$E = E^0_{(Cu^{2+}/Cu^+)} - 0.059 \log \frac{[Cu^+]}{[Cu^{2+}]} = 0.391\ V \quad (5)$$

where $E^0_{(Cu^{2+}/Cu^+)}$ = 0.153 V (see Table S1 in SI8 of the Supporting Information).[36] Strictly speaking, because the ionic strength is 0.7 M in this study, activity coefficients of different species should be included here for more precise calculation. However, a previous study reported that the discrepancy of calculated E values at an ionic strength of 0.50 M is less than 0.01 V.[27] Therefore, the employment of only concentrations of various species in the Nernst equation for rough estimation here is considered acceptable. Under the same conditions (at pH 8.0, with initial $[H_2Q]_0$ = 1.0 μM and $[Cu(I)]_0$ = 200 nM), a steady-state concentration of $[O_2^{\bullet -}]$ of ~10^{-13} M was predicted by the model, yielding the equilibrium redox potential of the system (on the basis of the $O_2/O_2^{\bullet -}$ couple).

$$E = E^0_{(O_2/O_2^{\bullet -})} - 0.059 \log \frac{[O_2^{\bullet -}]}{[O_{2(aq)}]} = 0.374\ V \quad (6)$$

Model-predicted concentrations of $SQ^{\bullet -}$ and HQ^- species were also employed to estimate the values of $E(SQ^{\bullet -}/HQ^-)$ using eq S-8 of the Supporting Information and E_h of the system as a function of time was measured, with results presented in Figure S10 in SI11 of the Supporting Information. The similarity between these model-predicted independent estimates of the system equilibrium redox potential and the measured E_h strongly supports the veracity of the model and the predicted $O_2^{\bullet -}$ and $SQ^{\bullet -}$ concentrations.

3.3. Implication of Findings. The kinetic model, using the single entities Cu(I) and Cu(II) to represent all cuprous and cupric species, was able to adequately describe the kinetics of Cu(I) oxidation and Cu(II) reduction in the presence of H_2Q in 0.7 M NaCl solution over the pH range of 6.5−8.0. We have presented evidence that Cu(II) is capable of catalyzing the oxidation of H_2Q under conditions typical of natural waters. The kinetic model indicated that the monoanion HQ^- is the active species responsible for reduction of Cu(II), with an intrinsic rate constant of $(5.0 \pm 0.4) \times 10^7\ M^{-1}\ s^{-1}$. While the semiquinone radical plays an important role as a chain-propagating species, the presence of O_2 in the system is also of particular importance in terms of supplying Cu(II) both by directly oxidizing Cu(I) and also through rapid oxidation of $SQ^{\bullet -}$ to generate $O_2^{\bullet -}$, the dominant oxidant of Cu(I). We have also shown that, at circumneutral pH, agreement between calculated half-cell reduction potentials of different redox couples involved in the modeled reactions provides confirmation of the veracity of the proposed kinetic model and associated rate constants, with the model providing critical insight into the thermodynamic and kinetic characteristics of quinone species and their interaction with copper under conditions typical of natural saline waters and intracellular environments.

dx.doi.org/10.1021/es4014344 | Environ. Sci. Technol. 2013, 47, 8355−8364

While a recent study by Uchimiya and Stone[73] indicated that the reduction of BQ by Fe(II) could be a vital process with regard to electron transport in suboxic and anoxic environments, the current work provides evidence that the oxidation of H_2Q by Cu(II) may play an important role in electron transfer under conditions typical of oxic natural saline waters. Further, it is recognized that quinone/hydroquinone moieties account for the redox properties of NOM, and as such, the results of this study have implications for the ability of NOM to induce oxidation state changes in copper species in natural aquatic systems. Additionally, the development of a kinetic model in which single entities Cu(I) and Cu(II) are used as representatives of all Cu(I) and Cu(II) species to overcome the difficulty of dealing with a large number of unknown kinetic constants should assist in understanding and predicting the factors controlling copper transformation, speciation, bioavailability, and toxicity in aquatic systems.

■ ASSOCIATED CONTENT

Ⓢ Supporting Information

Additional details on materials and methods, determination of rate constants, model sensitivity analysis, trace metal contamination, and turnover frequency calculation. This material is available free of charge via the Internet at http://pubs.acs.org.

■ AUTHOR INFORMATION

Corresponding Author

*Telephone: +61-2-9385-5059. Fax: +61-2-9313-8341. E-mail: d.waite@unsw.edu.au.

Notes

The authors declare no competing financial interest.

■ ACKNOWLEDGMENTS

Funding provided by the Australian Research Council Discovery Grant Scheme (DP0987188) is gratefully acknowledged as well as the award of an International Postgraduate Research Scholarship by The University of New South Wales to the lead author.

■ REFERENCES

(1) Yuan, X.; Pham, A. N.; Xing, G.; Rose, A. L.; Waite, T. D. Effects of pH, chloride, and bicarbonate on Cu(I) oxidation kinetics at circumneutral pH. *Environ. Sci. Technol.* **2011**, *46* (3), 1527−1535.

(2) González-Dávila, M.; Santana-Casiano, J. M.; González, A. G.; Pérez, N.; Millero, F. J. Oxidation of copper(I) in seawater at nanomolar levels. *Mar. Chem.* **2009**, *115* (1−2), 118−124.

(3) Sharma, V. K.; Millero, F. J. Oxidation of copper(I) in seawater. *Environ. Sci. Technol.* **1988**, *22* (7), 768−771.

(4) Sharma, V. K.; Millero, F. J. Effect of ionic interactions on the rates of oxidation of Cu(I) with O_2 in natural waters. *Mar. Chem.* **1988**, *25* (2), 141−161.

(5) Moffett, J. W.; Zika, R. G. Oxidation kinetics of Cu(I) in seawater: Implications for its existence in the marine environment. *Mar. Chem.* **1983**, *13* (3), 239−251.

(6) Moffett, J. W.; Zika, R. G. Measurement of copper(I) in surface waters of the subtropical Atlantic and Gulf of Mexico. *Geochim. Cosmochim. Acta* **1988**, *52* (7), 1849−1857.

(7) Uriu-Adams, J. Y.; Keen, C. L. Copper, oxidative stress, and human health. *Mol. Aspects Med.* **2005**, *26* (4−5), 268−298.

(8) Stern, B. R. Essentiality and toxicity in copper health risk assessment: Overview, update and regulatory considerations. *J. Toxicol. Environ. Health, Part A* **2010**, *73* (2−3), 114−127.

(9) Isaac, R. A.; Gil, L.; Cooperman, A. N.; Hulme, K.; Eddy, B.; Ruiz, M.; Jacobson, K.; Larson, C.; Pancorbo, O. C. Corrosion in drinking water distribution systems: A major contributor of copper and lead to wastewaters and effluents. *Environ. Sci. Technol.* **1997**, *31* (11), 3198−3203.

(10) Cech, I.; Smolensky, M. H.; Afshar, M.; Broyles, G.; Barczyk, M.; Burau, K.; Emery, R. Lead and copper in drinking water fountains—Information for physicians. *South. Med. J.* **2006**, *99* (2), 137−142.

(11) Slaats, P.; Brink, H.; van der Hoven, T. Copper corrosion control in the Netherlands. *Water Sci. Technol.: Water Supply* **2001**, *1* (3), 75−82.

(12) Ellingsen, D. G.; Horn, N.; Aaseth, J. Copper. In *Handbook on the Toxicology of Metals*, 3rd ed.; Nordberg, G. F., Fowler, B. A., Nordberg, M., Friberg, L. T., Eds.; Academic Press: San Diego, CA, 2007; pp 529−546.

(13) Linder, M. C. *Nutritional Biochemistry and Metabolism*; Elsevier: Amsterdam, The Netherlands, 1991.

(14) Navon, N.; Golub, G.; Cohen, H.; Meyerstein, D. Kinetics and reaction mechanisms of copper(I) complexes with aliphatic free radicals in aqueous solutions. A pulse-radiolysis study. *Organometallics* **1995**, *14* (12), 5670−5676.

(15) Balla, J.; Kiss, T.; Jameson, R. F. Copper(II)-catalyzed oxidation of catechol by molecular oxygen in aqueous solution. *Inorg. Chem.* **1992**, *31* (1), 58−62.

(16) Kamau, P.; Jordan, R. B. Kinetic study of the oxidation of catechol by aqueous copper(II). *Inorg. Chem.* **2002**, *41* (12), 3076−3083.

(17) Li, Y.; Trush, M. A. DNA damage resulting from the oxidation of hydroquinone by copper: Role for a Cu(II)/Cu(I) redox cycle and reactive oxygen generation. *Carcinogenesis* **1993**, *14* (7), 1303−1311.

(18) Li, Y.; Kuppusamy, P.; Zweier, J. L.; Trush, M. A. ESR evidence for the generation of reactive oxygen species from the copper-mediated oxidation of the benzene metabolite, hydroquinone: Role in DNA damage. *Chem.-Biol. Interact.* **1995**, *94* (2), 101−120.

(19) Li, Y. B.; Trush, M. A. Oxidation of hydroquinone by copper: Chemical mechanism and biological effects. *Arch. Biochem. Biophys.* **1993**, *300* (1), 346−355.

(20) Song, Y.; Buettner, G. R. Thermodynamic and kinetic considerations for the reaction of semiquinone radicals to form superoxide and hydrogen peroxide. *Free Radical Biol. Med.* **2010**, *49* (6), 919−962.

(21) Thorn, K. A.; Arterburn, J. B.; Mikita, M. A. ^{15}N and ^{13}C NMR investigation of hydroxylamine-derivatized humic substances. *Environ. Sci. Technol.* **1992**, *26* (1), 107−116.

(22) Uchimiya, M.; Stone, A. T. Reversible redox chemistry of quinones: Impact on biogeochemical cycles. *Chemosphere* **2009**, *77* (4), 451−458.

(23) Aeschbacher, M.; Graf, C.; Schwarzenbach, R. P.; Sander, M. Antioxidant properties of humic substances. *Environ. Sci. Technol.* **2012**, *46* (9), 4916−4925.

(24) Scott, D. T.; McKnight, D. M.; Blunt-Harris, E. L.; Kolesar, S. E.; Lovley, D. R. Quinone moieties act as electron acceptors in the reduction of humic substances by humics-reducing microorganisms. *Environ. Sci. Technol.* **1998**, *32* (19), 2984−2989.

(25) Paul, A.; Stösser, R.; Zehl, A.; Zwirnmann, E.; Vogt, R. D.; Steinberg, C. E. W. Nature and abundance of organic radicals in natural organic matter: Effect of pH and irradiation. *Environ. Sci. Technol.* **2006**, *40* (19), 5897−5903.

(26) Senesi, N.; Steelink, C. Application of ESR spectroscopy to the study of humic substances. In *Humic Substances*; Hayes, M. H. B., MacCarty, P., Malcolm, R. L., Swift, R. S., Eds.; John Wiley and Sons: Hoboken, NJ, 1989; pp 373−407.

(27) Uchimiya, M.; Stone, A. T. Redox reactions between iron and quinones: Thermodynamic constraints. *Geochim. Cosmochim. Acta* **2006**, *70* (6), 1388−1401.

(28) Nurmi, J. T.; Tratnyek, P. G. Electrochemical properties of natural organic matter (NOM), fractions of NOM, and model biogeochemical electron shuttles. *Environ. Sci. Technol.* **2002**, *36* (4), 617−624.

(29) Mandal, S.; Kazmi, N. H.; Sayre, L. M. Ligand dependence in the copper-catalyzed oxidation of hydroquinones. *Arch. Biochem. Biophys.* **2005**, *435* (1), 21−31.
(30) Millero, F. J.; Hershey, J. P.; Fernandez, M. The pK* of $TRISH^+$ in Na−K−Mg−Ca−Cl−SO_4 brines—pH scales. *Geochim. Cosmochim. Acta* **1987**, *51* (3), 707−711.
(31) Moffett, J. W.; Zika, R. G.; Petasne, R. G. Evaluation of bathocuproine for the spectro-photometric determination of copper(I) in copper redox studies with applications in studies of natural waters. *Anal. Chim. Acta* **1985**, *175*, 171−179.
(32) Zhou, M.; Diwu, Z.; Panchuk-Voloshina, N.; Haugland, R. P. A stable nonfluorescent derivative of resorufin for the fluorometric determination of trace hydrogen peroxide: Applications in detecting the activity of phagocyte NADPH oxidase and other oxidases. *Anal. Biochem.* **1997**, *253* (2), 162−168.
(33) Liu, T.; Li, X.; Waite, T. D. Depassivation of aged Fe^0 by inorganic salts: Implications to contaminant degradation in seawater. *Environ. Sci. Technol.* **2013**, *47* (13), 7350−7356.
(34) Johnson, K. A.; Simpson, Z. B.; Blom, T. Global Kinetic Explorer: A new computer program for dynamic simulation and fitting of kinetic data. *Anal. Biochem.* **2009**, *387* (1), 20−29.
(35) Ianni, J. C. *Kintecus, Version 3.9*, 2006; http://www.kintecus.com/.
(36) Moffett, J. W.; Zika, R. G. Reaction kinetics of hydrogen peroxide with copper and iron in seawater. *Environ. Sci. Technol.* **1987**, *21* (8), 804−810.
(37) Zafiriou, O. C.; Voelker, B. M.; Sedlak, D. L. Chemistry of the superoxide radical (O_2^-) in seawater: Reactions with inorganic copper complexes. *J. Phys. Chem. A* **1998**, *102* (28), 5693−5700.
(38) Pham, A. N.; Waite, T. D. Modeling the kinetics of Fe(II) oxidation in the presence of citrate and salicylate in aqueous solutions at pH 6.0−8.0 and 25 °C. *J. Phys. Chem. A* **2008**, *112* (24), 5395−5405.
(39) Rose, A. L.; Waite, T. D. Kinetic model for Fe(II) oxidation in seawater in the absence and presence of natural organic matter. *Environ. Sci. Technol.* **2002**, *36* (3), 433−444.
(40) Pham, A. N.; Rose, A. L.; Waite, T. D. Kinetics of Cu(II) reduction by natural organic matter. *J. Phys. Chem. A* **2012**, *116* (25), 6590−6599.
(41) Pham, A. N.; Xing, G.; Miller, C. J.; Waite, T. D. Fenton-like copper redox chemistry revisited: Hydrogen peroxide and superoxide mediation of copper-catalyzed oxidant production. *J. Catal.* **2013**, *301*, 54−64.
(42) Mel'nichenko, N.; Koltunov, A.; Vyskrebentsev, A.; Bazhanov, A. The temperature dependence of the solubility of oxygen in sea water according to the pulsed NMR data. *Russ. J. Phys. Chem. A* **2008**, *82* (5), 746−752.
(43) Williams, G. R. The reduction of cytochrome *c* by hydroquinone. *Can. J. Biochem. Phys.* **1963**, *41* (1), 231−237.
(44) Yamazaki, I.; Ohnishi, T. One-electron-transfer reactions in biochemical systems I. Kinetic analysis of the oxidation−reduction equilibrium between quinol−quinone and ferro−ferricytochrome *c*. *Biochim. Biophys. Acta* **1966**, *112* (3), 469−481.
(45) Rich, P. R.; Bendall, D. S. A mechanism for the reduction of cytochromes by quinols in solution and its relevance to biological electron transfer reactions. *FEBS Lett.* **1979**, *105* (2), 189−194.
(46) Peter, R. R. Electron transfer reactions between quinols and quinones in aqueous and aprotic media. *Biochim. Biophys. Acta* **1981**, *637* (1), 28−33.
(47) Rich, P. R.; Bendall, D. S. The kinetics and thermodynamics of the reduction of cytochrome *c* by substituted *p*-benzoquinols in solution. *Biochim. Biophys. Acta* **1980**, *592* (3), 506−518.
(48) Baxendale, J.; Hardy, H.; Sutcliffe, L. Kinetics and equilibria in the system ferrous ion + ferric ion + hydro-quinone + quinone. *Trans. Faraday Soc.* **1951**, *47*, 963−973.
(49) Miller, C. J.; Vincent Lee, S. M.; Rose, A. L.; Waite, T. D. Impact of natural organic matter on H_2O_2-mediated oxidation of Fe(II) in coastal seawaters. *Environ. Sci. Technol.* **2012**, *46* (20), 11078−11085.
(50) Miller, C. J.; Rose, A. L.; Waite, T. D. Hydroxyl radical production by H_2O_2-mediated oxidation of Fe(II) complexed by Suwannee River fulvic acid under circumneutral freshwater conditions. *Environ. Sci. Technol.* **2012**, *47* (2), 829−835.
(51) Miller, D. M.; Buettner, G. R.; Aust, S. D. Transition metals as catalysts of "autoxidation" reactions. *Free Radical Biol. Med.* **1990**, *8* (1), 95−108.
(52) Roginsky, V.; Barsukova, T. Kinetics of oxidation of hydroquinones by molecular oxygen. Effect of superoxide dismutase. *J. Chem. Soc., Perkin Trans. 2* **2000**, No. 7, 1575−1582.
(53) Patel, K. B.; Willson, R. L. Semiquinone free radicals and oxygen. Pulse radiolysis study of one electron transfer equilibria. *J. Chem. Soc., Faraday Trans. 1* **1973**, *69*, 814−825.
(54) Meisel, D. Free energy correlation of rate constants for electron transfer between organic systems in aqueous solutions. *Chem. Phys. Lett.* **1975**, *34* (2), 263−266.
(55) Diebler, H.; Eigen, M.; Matthies, P. Kinetische untersuchungen über die bildung von p-benzosemichinon aus chinon und hydrochinon in alkalischer lösung. *Z. Naturforsch., B: J. Chem. Sci.* **1961**, *16*, 629−637.
(56) Eyer, P. Effects of superoxide dismutase on the autoxidation of 1,4-hydroquinone. *Chem.-Biol. Interact.* **1991**, *80* (2), 159−176.
(57) Tatsumi, H.; Nakase, H.; Kano, K.; Ikeda, T. Mechanistic study of the autoxidation of reduced flavin and quinone compounds. *J. Electroanal. Chem.* **1998**, *443* (2), 236−242.
(58) Rao, P. S.; Hayon, E. Redox potentials of free radicals. IV. Superoxide and hydroperoxy radicals $\bullet O_2^-$ and $\bullet HO_2$. *J. Phys. Chem.* **1975**, *79* (4), 397−402.
(59) Morel, F. M. M.; Hering, J. G. *Principles and Applications of Aquatic Chemistry*; John Wiley and Sons: Hoboken, NJ, 1993.
(60) Wardman, P. The reduction potential of benzyl viologen: An important reference compound for oxidant/radical redox couples. *Free Radical Res.* **1991**, *14* (1), 57−67.
(61) Koppenol, W. H.; Stanbury, D. M.; Bounds, P. L. Electrode potentials of partially reduced oxygen species, from dioxygen to water. *Free Radical Biol. Med.* **2010**, *49* (3), 317−322.
(62) A. Roginsky, V.; M. Pisarenko, L.; Bors, W.; Michel, C. The kinetics and thermodynamics of quinone−semiquinone−hydroquinone systems under physiological conditions. *J. Chem. Soc., Perkin Trans. 2* **1999**, No. 4, 871−876.
(63) Bishop, C.; Tong, L. Equilibria of substituted semiquinones at high pH. *J. Am. Chem. Soc.* **1965**, *87* (3), 501−505.
(64) Roginsky, V. A.; Pisarenko, L. M.; Bors, W.; Michel, C.; Saran, M. Comparative pulse radiolysis studies of alkyl- and methoxy-substituted semiquinones formed from quinones and hydroquinones. *J. Chem. Soc., Faraday Trans.* **1998**, *94* (13), 1835−1840.
(65) Diebler, H.; Eigen, M.; Matthies, P. Chemische relaxation im redox-gleichgewicht chinon-hydrochinon. *Z. Elektrochem.* **1961**, *65* (7−8), 634−635.
(66) Millero, F. J.; Sharma, V. K.; Karn, B. The rate of reduction of copper(II) with hydrogen peroxide in seawater. *Mar. Chem.* **1991**, *36* (1−4), 71−83.
(67) Nohl, H.; Jordan, W. The involvement of biological quinones in the formation of hydroxyl radicals via the Haber−Weiss reaction. *Bioorg. Chem.* **1987**, *15* (4), 374−382.
(68) Zhu, B.-Z.; Zhao, H.-T.; Kalyanaraman, B.; Frei, B. Metal-independent production of hydroxyl radicals by halogenated quinones and hydrogen peroxide: An ESR spin trapping study. *Free Radical Biol. Med.* **2002**, *32* (5), 465−473.
(69) Kitagawa, S.; Fujisawa, H.; Sakurai, H. Scavenging effects of dihydric and polyhydric phenols on superoxide anion radicals, studied by electron-spin-resonance spectrometry. *Chem. Pharm. Bull.* **1992**, *40* (2), 304−307.
(70) Deeble, D. J.; Parsons, B. J.; Phillips, G. O.; Schuchmann, H.-P.; Von Sonntag, C. Superoxide radical reactions in aqueous solutions of pyrogallol and *N*-propyl gallate: The involvement of phenoxyl radicals. A pulse radiolysis study. *Int. J. Radiat. Biol.* **1988**, *54* (2), 179−193.

(71) Meisel, D.; Fessenden, R. W. Electron exchange and electron transfer of semiquinones in aqueous solutions. *J. Am. Chem. Soc.* **1976**, *98* (24), 7505−7510.
(72) Adams, G.; Michael, B. Pulse radiolysis of benzoquinone and hydroquinone. Semiquinone formation by water elimination from trihydroxy-cyclohexadienyl radicals. *Trans. Faraday Soc.* **1967**, *63*, 1171−1180.
(73) Uchimiya, M.; Stone, A. T. Reduction of substituted *p*-benzoquinones by Fe^{II} near neutral pH. *Aquat. Geochem.* **2010**, *16* (1), 173−188.
(74) Aeschbacher, M.; Vergari, D.; Schwarzenbach, R. P.; Sander, M. Electrochemical analysis of proton and electron transfer equilibria of the reducible moieties in humic acids. *Environ. Sci. Technol.* **2011**, *45* (19), 8385−8394.
(75) Gustafsson, J. *Visual MINTEQ, Version 2.61*; KTH Royal Institute of Technology: Stockholm, Sweden, 2009.